Crystal Structure Determination of Thymoquinone by High-Resolution X-Ray Powder Diffraction

S. Pagola,[1] A. Benavente,[2] A. Raschi,[2] E. Romano,[2] M.A.A. Molina,[2] and P.W. Stephens[3]

[1]Departamento de Fisicoquímica, Facultad de Ciencias Químicas, Universidad Nacional de Córdoba, Ciudad Universitaria, 5000, Córdoba, Argentina

[2]Facultad de Bioquímica, Química y Farmacia, Universidad Nacional de Tucumán, Ayacucho 471, 4000, Tucumán, Argentina

[3]Department of Physics and Astronomy, SUNY at Stony Brook, Stony Brook, NY 11789-3800

ABSTRACT

The crystal structure of 2-isopropyl-5-methyl-1,4-benzoquinone (thymoquinone) and its thermal behavior—as necessary physical and chemical properties—were determined in order to enhance the current understanding of thymoquinone chemical action by using high resolution x-ray powder diffraction, Fourier transform infrared spectroscopy (FTIR), and 3 thermo-analytical techniques thermogravimetric analysis (TGA), differential thermal analysis (DTA), and differential scanning calorimetry (DSC). The findings obtained with high-resolution x-ray powder diffraction and molecular location methods based on a simulated annealing algorithm after Rietveld refinement showed that the triclinic unit cell was a = 6.73728(8) Å, b = 6.91560(8) Å, c = 10.4988(2) Å, α = 88.864(2)°, β = 82.449(1)°, γ = 77.0299(9)°; cell volume = 472.52(1) Å^3, Z = 2, and space group $P\bar{1}$. In addition, FTIR spectrum revealed absorption bands corresponding to the carbonyl and C-H stretching of aliphatic and vinylic groups characteristically observed in such p-benzoquinones. Also, a chemical decomposition process starting at 65°C and ending at 213°C was noted when TGA was used. DSC allowed for the determination of onset at 43.55°C and a melting enthalpy value of ΔH_m = 110.6 J/g. The low value obtained for the fusion point displayed a van der Waals pattern for molecular binding, and the thermograms performed evidence that thymoquinone can only be found in crystalline triclinic form, as determined by DRX methods.

Corresponding Author: A. Benavente, Facultad de Bioquímica, Química y Farmacia. UNT. Ayacucho 471, San Miguel de Tucumán, Tucumán, 4000, Argentina; Tel: 0054-381-4247752-Int. 234; Fax: 0054-381-4311462; Email: albe@unt.edu.ar

INTRODUCTION

The seeds of *Nigella sativa L* (Black cumin)—widely grown in several third world countries in northern Africa and parts of Asia, as well as Saudi Arabia—are used as food seasoning in the Mediterranean region and, in some areas of India, in traditional medicine to treat a wide range of diseases including diarrhea and asthma.[1] Furthermore, in vitro antitumor activity,[2,3] together with various other therapeutic effects, has also been reported for *Nigella sativa L* oil, which contains nigellone and thymoquinone[4,5] in a concentration range of 18% to 24%, both of which are reported to be active principles of this seed oil.[6,7] Thymoquinone can also be found in other plants such as *Callitris quadrivalvis, Monarda fistulosa, Juniperus cedrus, Tetraclinis articulata,* and *Nepeta leucophylla*.

In addition, recent in vivo trials ascribe antitumoral properties to thymoquinone based on findings showing that thymoquinone in combination with ifosfamide (IFO) not only decreases the extent of renal damage but also enhances its anticancer outcome[8,9] in rats. Likewise, striking results have also been reported on thymoquinone's highly antioxidant potential corroborated in both isolated and synthesized thymoquinone[10] analyses. Moreover, thymoquinone has been shown to have a remarkable impact on the suppression of doxorubicin-induced renal diseases[11,12] in rats. Thus, all the pharmacological properties above mentioned render the analysis of thymoquinone structure relevant in order to enhance the understanding of its bioactivity.

The microcrystalline structure of thymoquinone was determined by means of high resolution x-ray powder diffraction. The simulated annealing and Rietveld refinement steps were repeated so as to furnish relevant data supporting the results obtained.

Thymoquinone powder samples were characterized by using thermoanalytical methods— thermogravimetric analysis (TGA), differential thermal analysis (DTA), and differential scanning calorimetry (DSC)—and FTIR spectroscopy. The

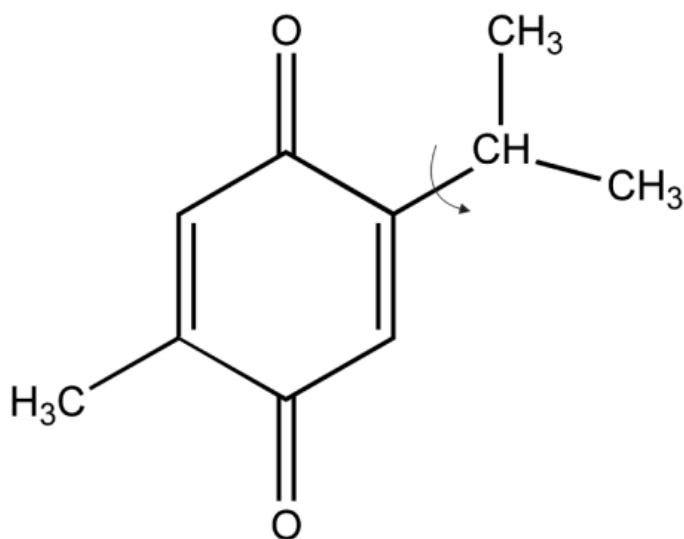molecule of thymoquinone obtained is illustrated in Figure 1.

Figure 1. The molecule of thymoquinone. Arrow shows the torsional degree of freedom.

MATERIALS AND METHODS

Thymoquinone (2-isopropyl-5-methyl-1,4-benzoquinone) powder was purchased from Sigma-Aldrich (St Louis, MO). TGA and DTA measurements of thymoquinone were performed with ATG-50 and ATD-50 Shimadzu equipment (Shimadzu, Kyoto, Japan). DSC data were collected using PerkinElmer Pyris 6 DSC equipment (PerkinElmer, Boston, MA). TGA and DTA measurements were performed with N_2 gas flux of 20 cm^3/min and a heating rate of 2°C/min starting at room temperature and ending at 250°C. DSC measurements were performed at the same heating rate but starting at 20°C and ending at 90°C.

The FTIR spectrum was performed by using a PerkinElmer 1600 spectrophotometer with a resolution of 2 cm^{-1}, and 64 scans in the spectral region between 4000 and 400 cm^{-1}. Thymoquinone powder was mixed with KBr and prepared as pellets.

High resolution x-ray powder diffraction data was collected at X3B1 beam line using the synchrotron at the National Synchrotron Light Source, Brookhaven National Laboratory, Upton, NY. The wavelength selected with a Si (111) double monochromator was 0.69940 Å. The wavelength was calibrated with a National Institute of Standards and Technology (NIST) Standard Reference Material 1976 Al_2O_3 plate. Incidental radiation intensity was monitored with an ion chamber, whereas diffracted intensity was measured with an NaI(Tl) scintillation detector. Likewise,

in-plane and out-of-plane resolutions of the diffractometer were defined by the use of a Ge (111) analyzer. The sample was slightly ground in a mortar and loaded into a 1.5-mm glass capillary. Powder diffraction data were collected at room temperature in the 2θ range 3.5° to 27.058° (*d* = 11.451-1.495 Å). First, the diffraction pattern[13-15] was indexed and the space group (or space group candidates) was determined. Estimates of the intensity of each Bragg peak were obtained by the Le Bail technique,[16] including estimates of correlations among overlapping peaks.[13] With the aim of obtaining a reasonable crystal density, the number of molecules in the irreducible cell (*Z*) was estimated using the molecular weight and the calculated cell volume. Furthermore, 3-dimensional molecular geometry was obtained either from similar structures containing the molecule or fragment of interest in database or was generated by semi-empirical or ab-initio calculations. A simulated annealing algorithm was used to obtain the location and conformation of the molecule in the unit cell so as to search for the best agreement between calculated and observed diffraction intensities for Bragg reflections[17] within the multidimensional configuration space.

RESULTS AND DISCUSSION

Crystal Structure Determination

The high resolution x-ray powder diffraction pattern was initially indexed with the TREOR[18] and ITO[19] (M_{20} = 62.8) programs. The crystal system obtained was triclinic and the reduced unit cell[20] (a = 6.739 Å, b = 6.932 Å, c = 10.501 Å, α = 88.59°, β = 82.43°, γ = 77.14°) was selected for further treatment of the diffraction data. Le Bail fits[16] were initially performed with the FULLPROF[21] program, which was repeated with the GSAS[22] program erify the accuracy of the unit cell obtained. This Le Bail fit allowed for a set of integrated intensities of the reflections. The agreement factors of the Le Bail fit were R_{wp} = 6.63%, χ^2 = 7.6.

Thymoquinone crystal structure was determined with the powder structure solution program (PSSP)[17] because it makes use of a specially defined figure of merit *S*, accounting for overlapping peaks.[13,17] Since the molecule structure studied was a simple one, only 1000 cycles per temperature were needed and only the 50 first reflections were used to solve the structure to a maximum 2θ of 14.745° (*d* = 2.725 Å).

Experience with organic molecules suggests Z = 2 yields a reasonable theoretical density of 1.15 g/cm^3. The potential space groups were $P1$ or $P\bar{1}$. Therefore, when the space group was $P\bar{1}$, the irreducible cell was $Z' = 1$, and the structure description and the simulated annealing search were performed with 7 parameters. Alternatively, 14 parameters

Table 1. Refined Crystallographic Parameters of Thymoquinone: Atomic Positions, Isotropic Thermal and Occupancy Factors of Non-Hydrogen Atoms*

Atom	x	y	Z	Ui/Ue*100	Occupancy
C1	0.989(6)	0.713(4)	0.352(5)	0.02(8)	1.0
C2	0.802(7)	0.692(5)	0.298(5)	0.02(7)	1.0
C3	0.627(6)	0.710(5)	0.377(5)	0.05(8)	1.23(9)
C4	0.612(7)	0.750(5)	0.515(5)	0.02(8)	1.0
C5	0.799(8)	0.772(5)	0.569(4)	0.03(8)	1.0
C6	0.974(7)	0.754(5)	0.489(5)	0.04(7)	1.23(9)
C7	0.820(9)	0.651(9)	0.157(5)	0.1(1)	1.23(9)
C8	0.80(2)	0.85(2)	0.08(2)	0.2(1)	1.6(2)
C9	0.67(2)	0.53(2)	0.12(1)	0.3(1)	1.6(2)
C10	0.78(1)	0.812(9)	0.710(4)	0.2(1)	1.6(2)
O1	1.153(7)	0.697(7)	0.283(5)	0.05(6)	1.0
O2	0.448(8)	0.766(7)	0.584(6)	0.04(6)	1.0

*$x, y, Z,$ are the atomic positions; UI/UE, isotropic thermal factor.

were necessary when the space group was $P1$ and the irreducible cell was $Z = 2$. The molecule of thymoquinone has one internal torsional degree of freedom (marked with an arrow in Figure 1).

Observations for Wilson statistics are too scanty to be useful in determining whether the cell is centro-symmetric, thus the solutions should be compared for both cases. Preliminary Rietveld refinements performed in crystal structure solutions yielded very similar S factors for space groups $P1$ and $P\bar{1}$. The observation of the Rietveld-refined atomic positions and the use of the PLATON Addsym[23] program (PLATON, Utrecht University, Utrecht, The Netherlands) suggested that the inversion symmetry missing (space group $P\bar{1}$) should be added.

Since a molecular location method was used to solve thymoquinone crystal structure, the choice of molecular geometry applied in the structure solution and the Rietveld refinement processes deserves further consideration.

Therefore, 2 approaches were attempted in order to choose an appropriate molecular geometry: (1) an initial sketch was optimized using the HyperChem (HyperGauss)[24] program, and (2) the Cambridge Structural Database[25] was consulted with the purpose of obtaining the geometries of similar molecular fragments. The 2,5-dimethyl-1,4-benzoquinone fragment was found in the entries CIKRAP, CISCOW, and DMEBQU. Since the 3 fragments encountered displayed similar bond lengths and angles, they were completed with the Chem3D[26] program to obtain 4 sets of molecular geometries for thymoquinone.

Consequently, 40 PSSP runs in the space group $P\bar{1}$ were performed for each one of the 4 geometry sets in order to select the molecular geometry of thymoquinone yielding the highest quality crystal structure solutions and Rietveld refinements. The best agreement factors obtained were $S = 0.096$, $S = 0.112$, $S = 0.114$, and $S = 0.123$ for DMEBQU,

CIKRAP, CISCOW, and HyperChem optimization, respectively.

Further refinements for the DMEBQU and CIKRAP solutions in $P\bar{1}$ were done using the Rietveld method and the GSAS[22] program. Such solutions generated almost equally good Rietveld refinements; the R_I factor of the DMEBQU solution being slightly smaller than the one reported in the present article.

Refinements were performed for scale factor, lattice parameters, 2θ zero point error, axial divergence asymmetry, peak shape and anisotropic strain profile parameters, atomic positions of non-Hydrogen atoms, occupancy factors (subjected to constraints), and isotropic thermal parameters. The background intensity was refined with a cosine Fourier series background function of the GSAS program. No background intensities were assumed a priori.

The position and orientation of the DMEBQU 2,5-dimethyl-1,4-benzoquinone fragment was refined as a rigid body. Two soft bond length constraints and one bond angle constraint were included to refine all atomic positions including the methyl carbons of the isopropyl group, with weight factor 1 in the last cycles of Rietveld refinement. The constraint values were chosen according to the distances and angles obtained in the molecular geometry optimization results using the HyperChem program.

The refined crystallographic parameters are shown in Table 1. The atomic positions and thermal and occupancy factors were corrected following the procedure described by Scott.[27] Despite the fact that the torsions of the 3 methyl groups were unable to be determined with the powder diffraction experiment used, an attempt was made to include hydrogen positions calculated with the WinGX[28] program, keeping non-Hydrogen atoms positions fixed; however, when thermal factors were refined, one of them became negative. Consequently, hydrogen atoms were left out in the final

Rietveld refinement. Similar to what has been reported in other publications,[29] the occupancy factors of the carbon atoms bonded to hydrogen were also refined subjected to constraints so that the CH_3 and CH groups had equivalent carbon occupancy factor values for each group. The occupancy factors of 3 methyl carbons, 1 tertiary carbon atom, and 2 carbons of the quinone ring were refined as well. The values obtained become significant when hydrogen atoms are omitted in the model; thus, once the number of missing hydrogen atoms in each group was accounted for, the expected occupancy values 1.23(9) for CH and 1.6(2) for CH_3 were relatively close to 1.17 and 1.5, respectively. The thermal factors were refined independently without constraints and are particularly large for the 3 methyl carbons and the tertiary carbon. This finding reflects in part the distribution of excess charge from the hydrogen atoms, which were not included in the structural model.

Figure 2 shows a plot of the refined diffraction pattern. The agreement factors were R_{wp} = 8.10%, R_I = 7.2%, and χ^2 = 11.3.
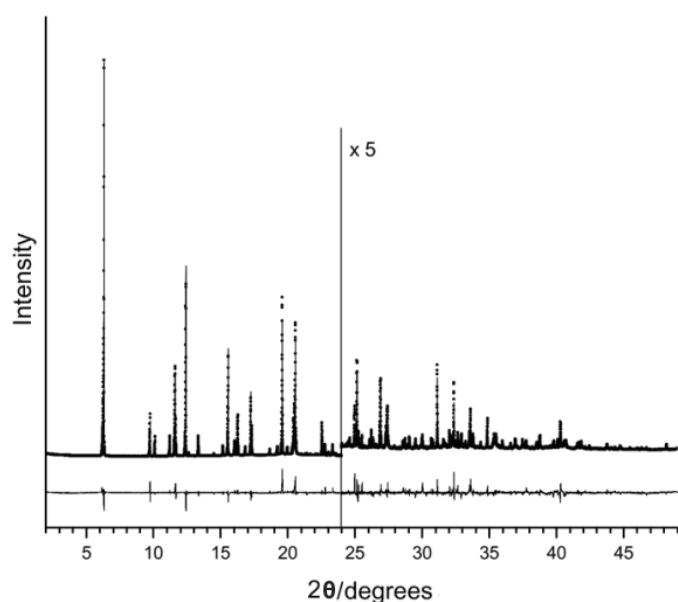

Figure 2. Rietveld refinement. Experimental data (dots), calculated pattern (solid line), and difference plot (bottom). Vertical ticks indicate allowed peak positions.

The representation of the unit cell along the [010] direction is shown in Figure 3A. The 2 molecules in the unit cell related by inversion symmetry belong to 2 sets of alternating molecular layers that pile up along the [010] direction, and parallel molecules between the same set of layers are separated by 6.916 Å. This feature can be seen in a representation of the crystal structure along the [001] direction (Figure 3B). The torsion angles are the following: C3-C2-C7-C9 = 29.0 grades and C3-C2-C7-C8 = -96.5 grades. Hydrogen

atom positions in the ring were unable to be determined unequivocally with high resolution x-ray powder diffraction data, therefore they are not included here. However, the occupancy factor for C atoms containing hydrogen was refined.
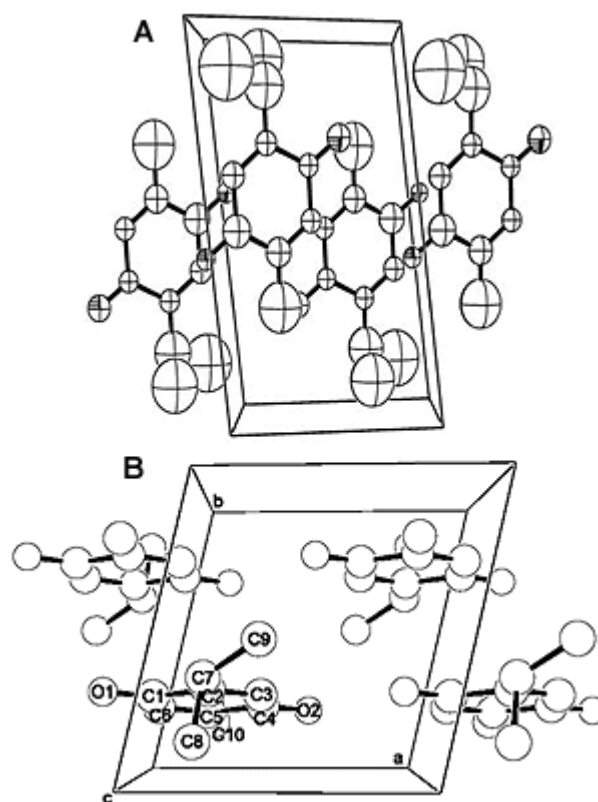

Figure 3. The crystal structure of thymoquinone view from the [010] direction (A); View from the [001] direction (B).

Thermal Analysis and Infrared Spectroscopy

A TGA measurement was performed to characterize the polycrystalline sample of thymoquinone. The chemical decomposition of the material (weight loss) started at 65°C and finished at ~213°C. Furthermore, the DTA experiment showed a sharp and well-defined endothermic peak centered at ~46.59°C—equivalent to the melting point of thymoquinone—followed by an endothermic broad band centered at 146.7°C, corresponding to the decomposition process, and ending at 160°C, which is produced in 1 step (Figure 4).

Figure 5 shows the acute endothermic peak obtained with DSC corresponding to the solid/liquid transition, with a change of enthalpy ΔH_m = 110.6 J/g. The onset obtained was 43.55°C, comparable to the fusion point experimentally determined by DTA.

The infrared spectrum of thymoquinone has been previously reported.[30] The spectrum obtained is shown in Figure 6. The
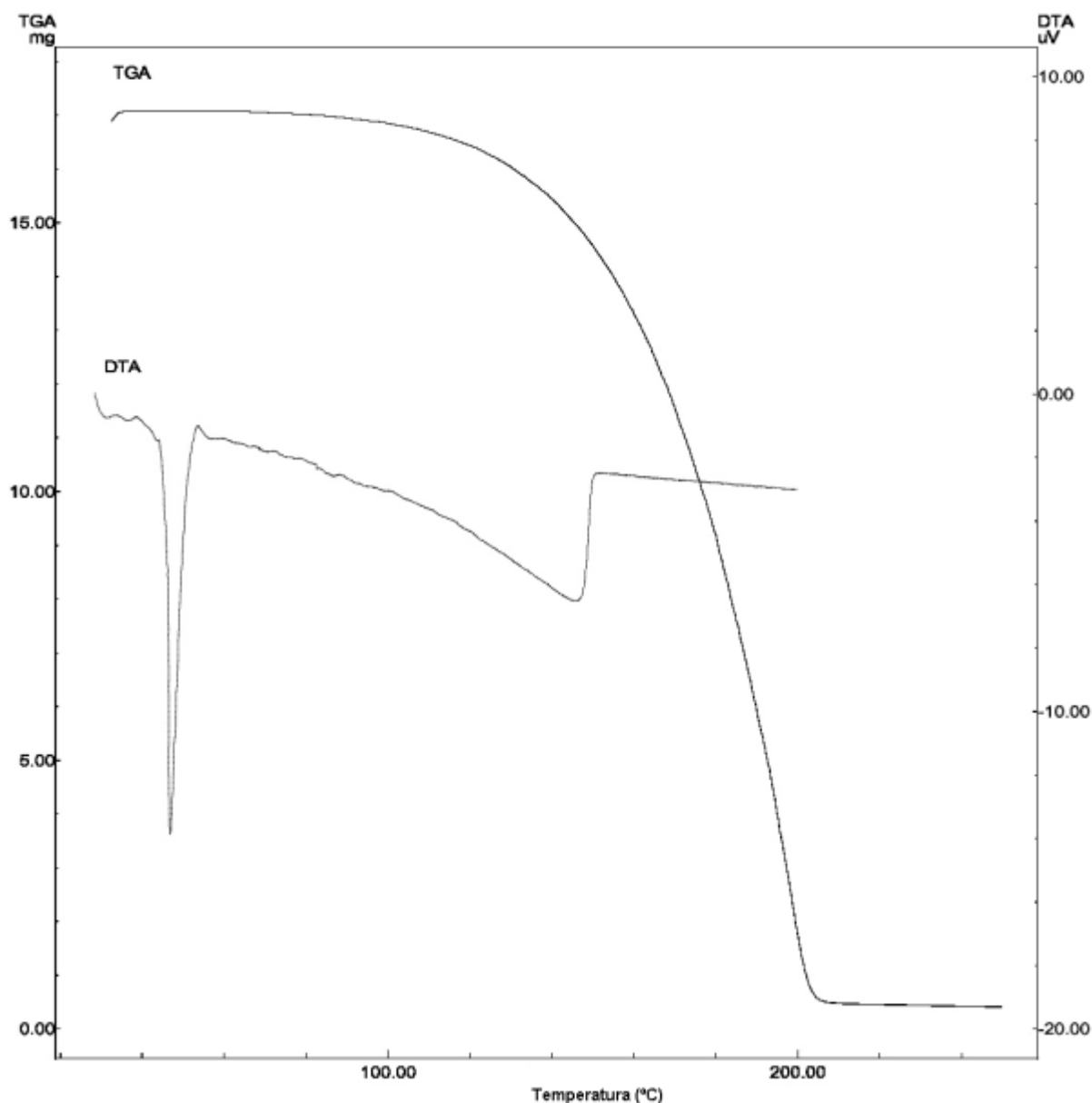
Figure 4. TGA and DTA thermograms for thymoquinone solid.

characteristic strong stretching band of the carbonyl group of a cyclohexadiene is observed at the wavenumber 1650cm^{-1}, which is supported by the values reported for thymoquinone (1.648 cm^{-1}) and 1,4 benzoquinone (1661cm^{-1}). The intense band present at 2967 cm^{-1} corresponds to the C-H stretching of aliphatic groups, and the value previously reported[30] was 2969 cm^{-1}. The weaker band observed at a higher wavenumber (~3040 cm^{-1}) was assigned to the stretching observed in the vinylic C-H in the C = C-H groups, which had previously been reported[30] at wavenumber 3041 cm^{-1}. This feature can be seen more clearly as an isolated band in the spectrum of 1,4-benzoquinone[31] (with-

out aliphatic C-H stretchings) at 3058 cm^{-1}. The C = C stretching (1640-1675 cm^{-1}) yielded an isolated and moderately strong band at 1640 cm^{-1} in 1,4-cyclohexadiene. The C = C stretching band cannot be unambiguously identified because the strong carboxylic stretching band in thymoquinone is present in this frequency range. In addition, the intensity of the C = C band is expected to be lower than both the carboxylic band and the C = C stretching in 1,4-cyclohexadiene, which contains no methyl and isopropyl substituents; however, it must be noted that there is a transition at 1673 cm^{-1} slightly separated from the carbonylic band (the same feature is present at 1678 cm^{-1} in 1,4-
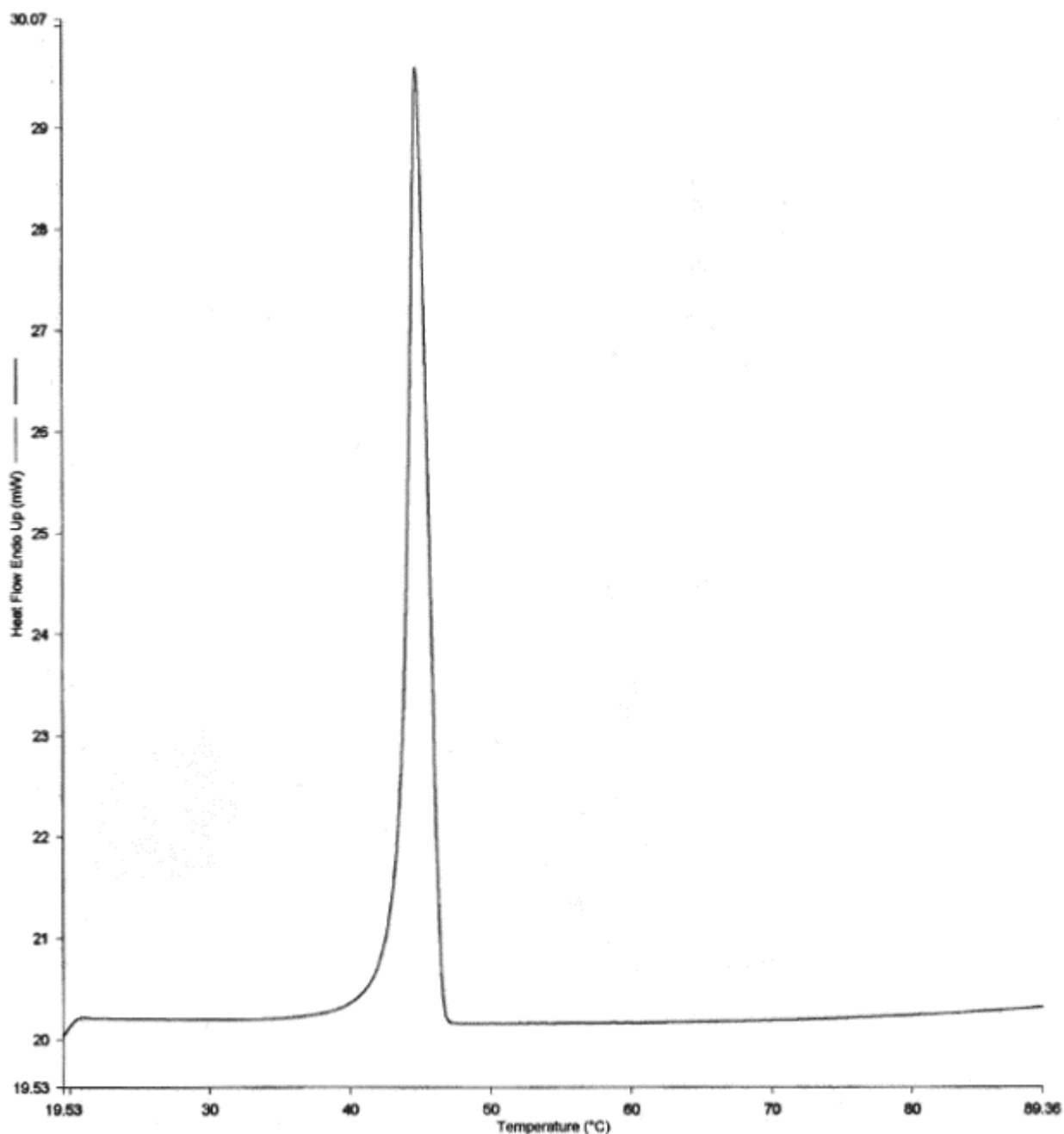
Figure 5. DSC thermograms for thymoquinone solid.

benzoquinone[31]) that could be tentatively ascribed to the C = C stretching band.

CONCLUSION

The studied crystal sample of thymoquinone was found to be present in the triclinic system. The asymmetric unit of thymoquinone ($Z = 2$) could be successfully located in space groups $P1$ and $P\bar{1}$ ($Z' = 1$).

The FTIR spectrum of thymoquinone showed typical absorption bands that could be assigned to carbonyl stretching and aliphatic and vinylic C-H stretchings.

The thermal analysis on thymoquinone supports the premise that weak van der Waals forces are present in the molecules of solid thymoquinone, and since no enthalpic change other than the change of state was observed, it is concluded that only 1 crystalline system exists in the studied sample.
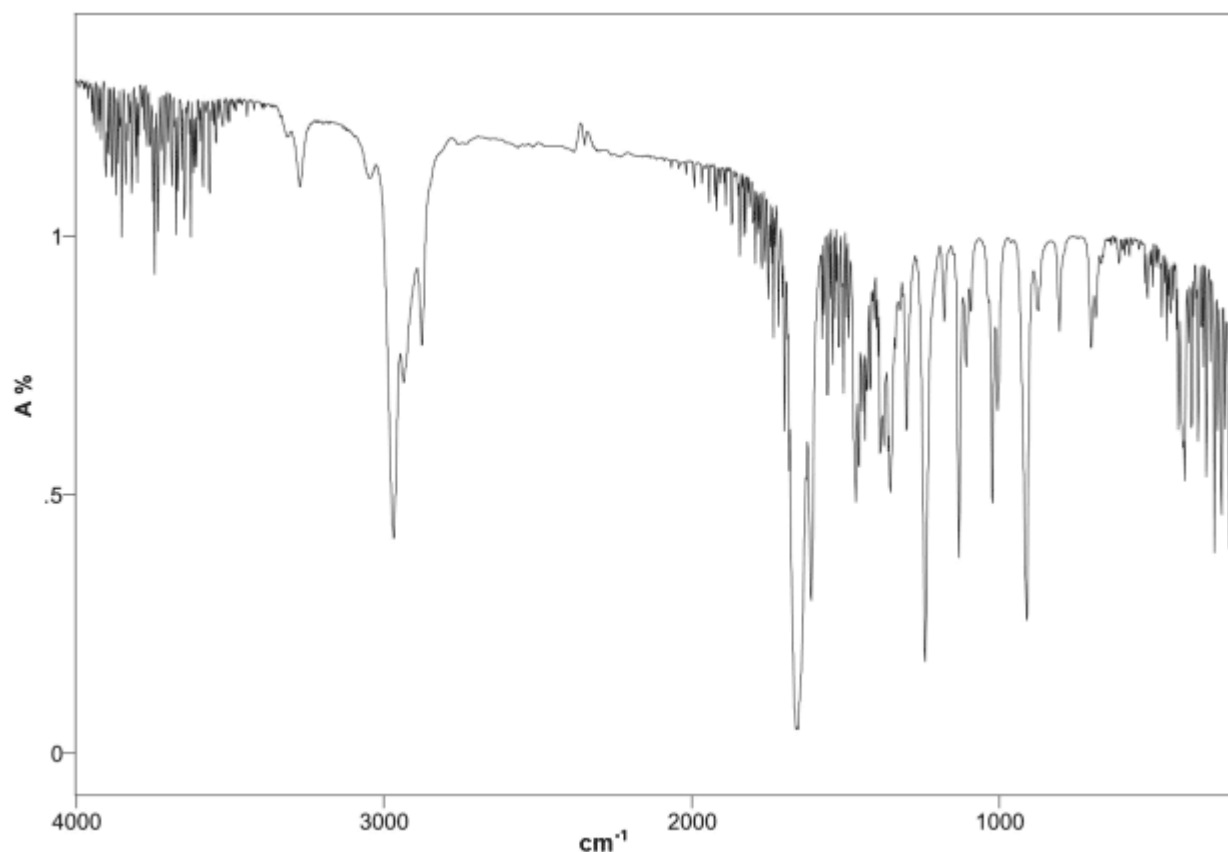
Figure 6. FTIR spectrum of thymoquinone solid.

REFERENCES

1. Gilani AH, Aziz N, Khurram IM, Chaudhary KS, Iqbal A. Bronchodilator, Spasmolytic and Calcium Antagonist Activities of *Nigella sativa* seeds (Kalonji): a traditional herbal product with Multiple Medicinal Uses. *J Pak Med Assoc*. 2001;51:115-119.

2. Salomi N, Nair S, Jayawardhanan K, Vorghese C, Pankkar K. Antitumour Principles from Nigella sativa seeds. *Cancer Lett*. 1992;63:41-46.

3. Worthen DR, Ghosheh OA, Crooks PA. The in vitro anti-tumor activity of some crude and purified components of blackseed, *Nigella sativa* Linn. *Anticancer Res*. 1998;18:1527-1532.

4. Houghton PJ, Zarka R, Delasheras B, Hoult JRS. Fixed oil of *Nigella sativa* and derived thymoquinone inhibit eicosanoid generation in leukocytes and membrane lipid-peroxidation. *Planta Med*. 1995;61:33-36.

5. Chakravarty N. Inhibition of Histamine release from mast cells by nigellone. *Ann Allergy*. 1993;70:237-242.

6. Abou Basha Alila I, Rashed Mohamed S, Aboul-Enein Asan Y. TLC assay of thymoquinone in black seed oil (*Nigella sativa* Linn) and identification of dithymoquinone and thymol. *J Liquid Chromatogr*. 1995;18:105-115.

7. Ghosheh OA, Houdi-AA, Crooks PA. High-performance liquid chromatographic analysis of the pharmacologically active quinines and related compounds in the oil of the black seed (*Nigella sativa* L). *J Pharm Biomed Anal*. 1999;19:757-762.

8. Badary OA. Thymoquinone attenuates ifosfamide-induced Fanconi syndrome in rats and enhances its antitumor activity in mice. *J Ethnopharmacol*. 1999;67:135-142.

9. Badary OA, Nagi MN, Al-Shabanah OA, Al-Sawaf HA, Al-Sohaibani MO, Al-Bekairi AM. Thymoquinone ameliorates the nephrotoxicity induced by cisplatin in rodents and potentiates its antitumor activity. *Can J Physiol Pharmacol*. 1997;75:1356-1361.

10. Milos M, Matelic J, Jerkovic I. Chemical composition and antioxidant effect of glycosidically bound volatile compounds from oregano (*Origanum vulgare L ssp hirtum*). *Food Chem*. 2000;71:79-83.

11. Badary O, Abdel-Naim A, Abdel-Wajab M, Hamada F. The influence of thymoquinone on doxorubicin-induced hyperlipidemic nephropathy in rats. *Toxicology*. 2000;143:3:219-226.

12. Al-Shabanah OA, Badary OA, Nagi MN, Al-Gharably NM, Al-Rikabi AC, Al-Bekairi AM. Thymoquinone protects against doxorubicin-induced cardiotoxicity without compromising its antitumor activity. *J Exp Clin Cancer Res*. 1998;17:193-198.

13. Pagola S, Stephens PW, Bohle DS, Kosar AD, Madsen SK. The structure of malaria pigment beta-haematin. *Nature*. 2000;404:307-310.

14. Shankland K, McBride L, David WIF, Shankland N, Steele G. Molecular, crystallographic and algorithmic factors in structure determination from powder diffraction data by simulated annealing. *J Appl Crystallogr*. 2002;35:443-454.

15. Engel GE, Wilke S, Konig O, Harris KDM, Leusen FJJ. Powder Solve – a complete package for crystal structure solution from powder diffraction patterns. *J Appl Crystallogr*. 1999;32:1169-1179.

16. Le Bail A, Duroy H, Fourquet JL. *Ab-initio* structure determination of LiSbWO$_6$ by X-ray powder diffraction. *Mater Res Bull*. 1988;23:447-452.

17. Stephens PW, Pagola S. *Powder Structure Solution Program*. Available at: http://powder.physics.sunysb.edu. Accessed March 27, 2004.

18. Werner PE, Eriksson L, Westdahl M. TREOR, a semiexhaustive trial-and-error powder indexing program for all symmetries. *J Appl Crystallogr*. 1985;18:367-370.

19. Visser JW. A fully automatic program for finding the unit cell from powder data. *J Appl Crystallogr*. 1969;2:89-95.

20. Krivy I, Gruber B. A unified algorithm for determining the reduced (Niggli) cell. *Acta Crystallogr*. 1976;A32:297-298.

21. Rodriguez-Carvajal J. FULLPROF: A program for Rietveld refinement and pattern matching analysis. Abstracts of the Satellite Meeting on Powder Diffraction of the XV Congress of the IUCr. 1990; Toulouse, France; 127.

22. Larson AC, Von Dreele RB. *GSAS–Generalized Crystal Structure Analysis System*. Los Alamos, NM: Los Alamos National Laboratory; 1987. Report No. LA-UR-86-748.

23. Spek AL. *PLATON - A Multipurpose Crystallographic Tool* [computer program]. 1990; Available at: http://www.cryst.chem.uu.nl/platon. Accessed March 22, 2004.

24. *HyperChem Molecular Modeling System* [computer program]. Version 6.01. Gainesville, FL: Hypercube Inc; 2000.

25. Allen FH, Kennard O. 3D Search and Research using the Cambridge Structural Database. *Chemical Design Automation News*. 1998;8:31-37.

26. *CS Chem 3D Pro Molecular Modeling and Analysis Program* [computer program]. Cambridge, MA: CambridgeSoft Corp; 1996.

27. Scott HG. The estimation of standard deviation in powder diffraction Rietveld Refinements. *J Appl Crystallogr*. 1983;16:159-163.

28. Farrugia LJ. WinGX suite for small-molecule single-crystal crystallography. *J Appl Crystallogr*. 1999;32:837-838.

29. Dinnebier RE, Dollase WA, Helluv X, et al. Order-disorder phenomena determined by high-resolution powder diffraction: the structures of tetrakis (trimethylsilyl) methane C[Si(CH$_3$)$_3$]$_4$ and tetrakis (trimethylsilyl) silane Si[Si(CH$_3$)$_3$]$_4$. *Acta Crystallogr*. 1999;B55:1014-1029.

30. Integrated Spectral Data Base System for Organic Compounds [database online]. Ibaraki, Japan: National Institute of Advanced Industrial Science and Technology; 2003. Updated September 30, 2003. Available at: http://www.aist.go.jp/RIODB/SDBS/menu-e.html.

31. Yamakita Y, Tasumi M. Vibrational analyses of p-benzoquinodimethane and p-benzoquinone based on *ab initio* Hartree-Fock and second-order Moller-Plesset calculations.*J Phys Chem*. 1995;99:8524-8534.